Iranian Journal of Basic Medical Sciences
ijbms.mums.ac.ir

Time-dependent modulation of FXR and Nrf2 signaling in rat models of BDL-induced cholestasis

Seyed Ebrahim Daryabari [1#], Elmira Jafari Afshar [2#], Azadeh Khalili [1, 3], Seyed Ali Hashemi [4], Parham Samimisadeh [2], Gholamreza Bayat [3*], Hossein Karim [2, 5*]

[1] Evidence-based Phytotherapy and Complementary Medicine Research Center, Alborz University of Medical Sciences, Karaj, Iran
[2] Cardiovascular Research Center, Alborz University of Medical Sciences, Karaj, Iran
[3] Department of Physiology-Pharmacology-Medical Physics, School of Medicine, Alborz University of Medical Sciences, Karaj, Iran
[4] Department of Pathology, School of Medicine, Alborz University of Medical Sciences, Karaj, Iran
[5] Department of Cardiology, School of Medicine, Alborz University of Medical Sciences, Karaj, Iran

ARTICLE INFO

Article type:
Original

Article history:
Received: Jul 31, 2025
Accepted: May 6, 2026

Keywords:
Bile duct ligation (BDL)
Cholestasis
Cholestatic liver injury
Farnesoid X receptor
Nuclear factor erythroid 2-related factor 2

ABSTRACT

Objective(s): Farnesoid X receptor (FXR) and nuclear factor erythroid 2-related factor 2 (Nrf2) protect the liver against cholestatic injury by regulating antioxidant and anti-inflammatory pathways. Bile duct ligation (BDL) is a standard model for studying cholestatic liver disease, yet the temporal dynamics of FXR/Nrf2 signaling and their downstream mediators remain unclear. To investigate time-dependent changes in hepatic FXR, Nrf2, and downstream effectors over six weeks following BDL in rats, to identify potential preventive and therapeutic targets.

Materials and Methods: Forty-nine male Wistar rats were divided into one sham-operated group and six BDL groups, sacrificed sequentially from weeks 1 to 6 post-surgery. Biochemical assays, histopathology, and molecular analyses were performed to assess dynamic changes in FXR, Nrf2, and related oxidative stress and inflammatory markers.

Results: The most severe histological distortions were observed mainly at week six. Expression reductions in FXR, Superoxide Dismutase (SOD), Alpha-Glutathione S-Transferase (α-GST), and Glutamate-Cysteine Ligase Modifier Subunit (GCLM) were notable from week 1 to week 6, significantly declining in BDL rats compared to sham-operated ones. Nrf2 notably decreased at week 4 post-BDL (*P-value*<0.05). TNF-α exhibited an increasing trend, peaking at week 6 (*P*<0.001). FXR prominently decreased in weeks 1 and 5 (*P*<0.001), and SOD notably decreased in week 5 (*P*<0.05). α-GST and GCLM also markedly decreased, especially during BDL-W3 and BDL-W4 (*P*<0.001).

Conclusion: Temporal suppression of FXR/Nrf2 signaling and antioxidant defenses likely contribute to BDL-induced cholestatic injury, with a biphasic pattern across acute and sub-acute phases. These pathways may serve as therapeutic targets during disease progression.

▶ Please cite this article as:
Daryabari SE, Jafari Afshar E, Khalili A, Hashemi SA, Samimisadeh P, Bayat Gh, Karim H. Time-dependent modulation of FXR and Nrf2 signaling in rat models of BDL-induced cholestasis. Iran J Basic Med Sci 2026; 29: 1012-1019. doi: https://dx.doi.org/10.22038/ijbms.2026.90035.19420

Introduction

Cholestatic liver injury represents a potential precursor to liver failure and cirrhosis, with diverse triggers encompassing bile acids, genetic defects, mechanical abnormalities, toxins, and immunological dysregulation (1). Bile acids, in particular, can incite an inflammatory response within hepatocytes, manifesting in symptoms and complications, including jaundice, pruritus, and fatigue (2, 3). In more severe instances, cholestasis can move into cirrhosis, marked by extensive fibrosis and the distortion of normal liver architecture (4). The progression to cirrhosis may culminate in liver failure and associated complications, such as portal hypertension, esophageal varices, and hepatocellular carcinoma. Understanding the intricate mechanisms underlying cholestatic liver injury is imperative for advancing preventive and therapeutic strategies in clinical practice (1, 2).

The Farnesoid X receptor (FXR) and Nuclear factor erythroid 2-related factor 2 (Nrf2) pathways play essential roles in protecting against cholestatic liver damage by regulating oxidative stress and inflammation (3). Activating Nrf2 has been shown to inhibit oxidative stress and inflammation, regulate bile acid levels, and reduce fibrosis in the liver (5). On the other hand, decreased activity of FXR, especially during an autophagy deficiency, can contribute to cholestasis and liver injury (5, 6). Elevated bile acids can cause neutrophil-mediated inflammation in the liver, leading to hepatocyte damage (3). Nrf2 regulates oxidative stress by enhancing essential antioxidants, including Superoxide Dismutase (SOD), Glutathione

**Corresponding authors:* Gholamreza Bayat. Department of Physiology, Pharmacology, and Medical Physics, School of Medicine, Alborz University of Medical Sciences, West Bu-Ali Street, Karaj, Alborz Province, Iran. Tel: +98-2634198302, Fax: +98-2634287425, Email: g.bayat@abzums.ac.ir; Hossein Karim. Cardiovascular Research Center, Alborz University of Medical Sciences, Karaj, Iran, Department of Cardiology, School of Medicine, Alborz University of Medical Sciences, Karaj, Iran. Tel: +98-2634552001, Fax: +98-2634554484, Email: h.karim@abzums.ac.ir
# These authors contributed equally to this work

(GSH), Alpha-Glutathione S-Transferase (α-GST), and Glutamate-Cysteine Ligase (GCL)(7). GCL is a protein complex consisting of two distinct subunits: a catalytic subunit (GCLC) and a modulatory subunit (GCLM)(8). Altered GSH levels are linked to cirrhosis (9). Research notes reduced SOD activity in liver cirrhosis, contributing to damage (10). Despite extensive research in cholestatic liver disease, a significant gap remains in understanding the molecular mechanisms of antioxidant pathways in oxidative stress during cholestasis, including the roles of FXR, Nrf2, GCL, GST, and SOD (11). Limited knowledge exists of preventive strategies and treatments, especially in the early stages (12). Recent studies suggest that targeting FXR agonists may be a potential treatment approach for cholestatic liver diseases, such as primary biliary cholangitis and primary sclerosing cholangitis, by modifying bile acid metabolism and reducing inflammation (6). Understanding how these pathways interact and affect cholestatic liver injury is essential for developing effective prevention and treatment strategies (12, 13).

To identify potential therapeutic targets for cholestatic liver disease, we investigated the temporal expression of FXR, Nrf2, GCLM, αGST, SOD, and tumor necrosis factoralpha (TNFα) in liver tissues of rats subjected to BDL over six weeks, focusing on dynamic gene expression changes during disease progression.

Materials and Methods

Animals

Forty-nine male Wistar rats, aged eight weeks and weighing between 230 and 250 grams, were obtained from the Royan Animal Breeding Center in Karaj, Iran. These rats were housed in standardized conditions, maintaining a controlled room temperature of 22±2 ˚C, a 12-hour light/dark cycle, and a relative humidity range of 40%-60%. They had unrestricted access to food and water throughout the study. All animal care and experimental procedures adhered to national guidelines and were approved by the Research Ethics Committee of Alborz University of Medical Sciences. These procedures followed the principles outlined in the National Institute of Health Guide for the Care and Use of Laboratory Animals (IR.Abzums.REC.1400.114).

Experimental protocol

The study encompassed a control group and a sham-operated group as non-BDL groups and six distinct experimental BDL groups, each group comprising seven animals. The BDL groups were specifically designated as BDL-W1 to BDL-W6, denoting the length of time between the BDL procedure and sacrifice, ranging from one to six weeks.

Experimental design

The surgical procedure was conducted under sterile conditions, utilizing high-magnification surgical loupes and specialized microsurgical tools. The animals received deep surgical anesthesia through a single intraperitoneal (IP) injection of ketamine (60 mg/kg)(Alfasan; Woerden, Holland) and xylazine (8 mg/kg)(Alfasan; Woerden, Holland), ensuring they were completely relaxed and insensitive to pain throughout the process. Following the induction of anesthesia, the bile duct was carefully isolated and ligated using a method previously described by Yang *et al* (14). In brief, a midline incision was made, and the bile duct was gently separated from the surrounding tissue. Two ligatures were applied to the bile duct using 4-0 silk (SUPA Medical Devices Co., Iran) sutures; the first ligature was placed near the junction of the hepatic ducts, while the second ligature was positioned above the entrance of the pancreatic duct. To prevent reconnection, the duct was cut between the two ligatures. The sham-operated group underwent a similar procedure, except that the bile duct was not ligated. Throughout the surgery and recovery period, the animals' body temperatures were closely monitored and maintained within a normal range of 37±0.5 ˚C. Once the surgery was complete, the abdominal wall and skin incisions were closed using absorbable (3-0 catgut)(SUPA Medical Devices Co., Iran) and non-absorbable (3-0 silk) (SUPA Medical Devices Co., Iran) sutures, respectively. The animals were then moved to individual cages for recovery. During the initial post-operative week, the wounds were kept clean and infection-free with topical applications of tetracycline ointment 3% (Iran-Najo. Co., Iran).

Biochemical analysis

At the end of the experimental protocol, the animals were deeply anesthetized with IP injection of ketamine (60 mg/kg) and xylazine (8 mg/kg). A midline laparotomy was performed to expose the abdominal organs. After performing thoracotomy and exposure of the heart, approximately 5 mL of blood was collected from the right ventricle for biochemical analysis of liver enzymes, including aspartate transaminase (AST), alanine transaminase (ALT), lactate dehydrogenase (LDH), and alkaline phosphatase (ALP), using Pars Azmun commercial kits (Pars Azmun Co, INC, Karaj, Iran), according to the manufacturer's guidelines.

Histopathological examination

The right lobe of each liver was excised and promptly fixed in a 10% formalin solution. The samples then underwent sample preparation for microscopic study, which consisted of fixation, dehydration, embedding, and staining. The fixation process involved a paraffin-based method, followed by dehydration in gradually increasing ethanol concentrations. Next, the samples were embedded in paraffin wax and sectioned using standard histological techniques. The paraffin blocks were then cut into sections of 5 µm thickness. Finally, the slides were stained with hematoxylin and eosin (H&E), and reticulin stains to enhance their microscopic features. Histological changes were scored as none (0), active damage less than 25% (1), active damage less than 50% (2), active damage less than 75% (3) damage, and active damage more than 75% (4).

Quantitative real-time reverse-transcription PCR (qRT-PCR) assessment

To determine the expression of liver FXR, Nrf2, GCLM, α-GST, SOD, and TNF-α, real-time qRT- PCR was conducted following a standard protocol. First, approximately 30 mg of right hepatic lobe tissue was homogenized using a DAIHAN-brand homogenizing stirrer (HS-30E; Korea). Subsequently, Trizol (Yekta Tajhiz Azma Co., Iran) was employed to extract the RNA according to the manufacturer's guidelines. Following the manufacturer's instructions, reverse transcription was performed utilizing a Yekta Tajhiz Azma cDNA synthesis kit (Tehran, Iran).

The expression levels of the target genes were quantified via Real-Time PCR using SYBR green (Yekta Tajhiz Azma Co., Iran). Each Experiment was performed in duplicates as follows: consisting of an initial denaturation step at 95 ˚C for 10 min, followed by 45 cycles of 95 ˚C for 10 sec, 60 ˚C for 10 sec, and 72 ˚C for 10 sec. Gene expression was normalized against GAPDH and presented as fold change. The gene-specific primers used are listed in Table 1.

Primers used for quantitative realtime PCR were selected based on previously published studies investigating the respective target genes in rat models. The corresponding gene sequences were verified using the NCBI GenBank database to ensure specificity for the rat genome. Primer design parameters, including melting temperature ™, GC content, and the avoidance of secondary structures and primer–dimer formation, were carefully considered. All primers were commercially synthesized by Metabion (Germany).

Statistical analysis

The data, excluding histological findings, were presented as mean±SEM. Inter-group comparisons were conducted using one-way ANOVA. Subsequently, the Tukey test was employed as a *post hoc* analysis to identify specific variations between means whenever significance was detected. The median and interquartile range (IQR) were used to analyze histological data subjected to the Kruskal-Wallis nonparametric test. A significance level of $P<0.05$ was adopted. Graphical representations were generated using GraphPad Prism version 8.0.2 (GraphPad Software, San Diego, CA, USA).

Results

Since their values were statistically indistinguishable, the Sham-operated group has been used interchangeably with the control group to prevent the repetition of identical data.

Liver and body weights

The ratio of liver weight to the animal's body weight is shown in Table 2. Liver weight to body weight ratio showed a nonsignificant increase in the experimental groups compared to the sham-operated group. Notably, the BDL-W3 group had a significantly higher ratio than the sham-operated group ($P<0.001$). Additionally, when we compared the experimental groups, the increase in this ratio was statistically significant in the BDL-W3 group compared to the BDL-W1 and BDL-W2 groups ($P<0.05$ and $P<0.05$, respectively). Conversely, a notable decline in this ratio was observed in the BDL-W4 to W6 groups when contrasted with the third-week group ($P<0.05$, $P<0.05$, and $P<0.01$, respectively).

Table 1. Nucleotide sequences of forward and reverse primers used for qPCR analysis of target genes

Genes	Primer sequences (5′-3′)	
	Forward	Reverse
FXR	GCCGTGTACAAGTGTAAGAAC	AGCCGTTTAGATTTACACTGG
Nrf2	AGTGGATCTGTCAGCTACTC	GGGAATGTCTCTGCCAAAAG
SOD	TGTGTCCATTGAAGATCGTG	TCCAGCATTTCCAGTCTTTG
α-GST	GTGGAGATTGATGGGATGAAG	GGGAATGTAAGGGTAATGGAG
GCLM	GACAAAACACAGTTGGAGCAG	GGTCATTGTGAGTCAGTAGCTG
TNF-α	TCTGTCTACTGAACTTCGGG	TGATCTGAGTGTGAGGGTC
GAPDH	GCCTTCTCTTGTGACAAAGTG	CTTCCCATTCTCAGCCTTG

Table 2. Effect of bile duct ligation on rats' body and liver weights

Groups	Final body weights (Gram)	Final liver weights (Gram)	Liver weight/body weight
Sham-Operated	346.5±17.01	13.60±0.76	39.50±1.89
BDL-W1	255.2±8.94	13.00±0.77	51.20±2.88
BDL-W2	284.7±17.79	14.80±1.07	52.20±2.88
BDL-W3	250.2±15.8	18.40±2.44	72.20±7.21$^{***\,\$}$
BDL-W4	249.4±15.14	12.60±1.53	50.00±4.49$^{\#}$
BDL-W5	258.9±8.23	13.30±1.69	50.80±5.53$^{\#}$
BDL-W6	291.5±15.85	13.10±1.59	44.70±4.18$^{\#\#}$

Data were presented as mean±SEM in the sham-operated and 6 experimental groups (n=7), including bile duct ligation (BDL) for 1 to 6 weeks which are abbreviated as BDL-W1, BDL-W2, BDL-W3, BDL-W4, BDL-W5, and BDL-W6
$^{***}P<0.001$ vs Sham-operated group, $^{\dagger}P<0.05$ vs BDL-W1 group, $^{\$}P<0.05$ vs BDL-W2 group, $^{\#}P<0.05$, $^{\#\#}P<0.01$ vs BDL-W3 group

Biochemical results

Serum levels of liver enzymes have been reported in Table 3. Compared to the sham-operated group, serum levels of AST were significantly higher in all experimental groups, including BDL-W1 to BDL-W6 ($P<0.05$, $P<0.05$, $P<0.001$, $P<0.001$, $P<0.001$, and $P<0.001$, respectively). Moreover, Comparative analysis between various BDL subgroups demonstrated that compared to that of the BDL-W1 and W2 groups, the serum level of AST was significantly higher in the BDL-W4 ($P<0.05$ and $P<0.05$), W5 ($P<0.001$ and $P<0.001$) and W6 ($P<0.001$ and $P<0.001$), respectively. The most elevation in the AST serum level was also seen after four weeks of bile duct ligation, so compared to BDL-W3, AST level significantly elevated in BDL-W5 ($P<0.05$) and W6 ($P<0.05$), respectively. There was no significant difference was observed among BDL-W4, BDL-W5, and BDL-W6 in this regard.

In a similar pattern, compared to the sham-operated group, the serum levels of ALT were also significantly elevated in all BDL groups from BDL-W1 to BDL-W6 ($P<0.05$, $P<0.05$, $P<0.001$, $P<0.001$, $P<0.001$, and $P<0.05$,

Table 3. Effect of rat bile duct ligation on serum levels of liver function tests and cellular damage markers

Groups	AST (IU/L)	ALT (IU/L)	LDH (IU/L)	ALP (IU/L)
Sham-Operated	144.8±10.1	109.5±9.0	328.0±23.0	356.5±24.3
BDL-W1	346.8±52.9*	183.0±17.5*	619.8±51.6**	990.3±78.1***
BDL-W2	306.3±49.8*	159.8±18.8*	860.4±70.8$^{***\diamond}$	796.8±45.4**
BDL-W3	445.5±37.9***	242.3±20.0$^{***\$}$	296.3±27.6$^{\dagger\dagger\dagger\$\$\$}$	945.2±78.9***
BDL-W4	534.6±47.1$^{***\$}$	223.9±18.8***	447.8±50.9$^{\dagger\$\$\$}$	947.8±55.6***
BDL-W5	633.3±64.8$^{***\dagger\dagger\dagger\$\$\$\wr}$	224.6±16.6***	350.4±34.8$^{\dagger\dagger\$\$\$}$	843.1±95.9***
BDL-W6	657.2±18.5$^{***\dagger\dagger\dagger\$\$\$\wr}$	196.3±15.8*	359.0±30.1$^{\dagger\dagger\$\$\$}$	787.8±34.3**

Data were presented as mean±SEM in the sham-operated and 6 experimental groups (n=7), including bile duct ligation (BDL) for 1 to 6 weeks which are abbreviated as BDL-W1, BDL-W2, BDL-W3, BDL-W4, BDL-W5, and BDL-W6.
$^{*}P<0.05$, $^{**}P<0.01$, $^{***}P<0.001$ vs Sham-Operated group, $^{\dagger}P<0.05$, $^{\dagger\dagger}P<0.01$, $^{\dagger\dagger\dagger}P<0.001$ vs BDL-W1 group, $^{\$}P<0.05$, $^{\$\$\$}P<0.001$ vs BDL-W2 group, $^{\#}P<0.05$ vs BDL-W3 group
AST: Aspartate aminotransferase, ALT: Alanine aminotransferase, LDH: Lactate dehydrogenase, ALP: Alkaline phosphatase, IU/L: International Units per Liter

Table 4. Effect of rat Bile duct ligation on histological changes in Hematoxylin and Eosin (H&E) and reticulin-stained liver sections

	Histological indices	Sham-operated	BDL-W1	BDL-W2	BDL-W3	BDL-W4	BDL-W5	BDL-W6
	Liver histology: H&E staining							
1	Vascular congestion	0	1(0)	1(0)	1(0)	1(0.5)	2(1)**	3(1.25)$^{***\dagger\$\#}$
2	Sinusoidal dilation	0	0.5(1)	1(0)	1.5(1)*	1(1.25)	1(0)	3(2)$^{***\dagger\dagger\#}$
3	Lymphocytic infiltration	0	1(1)	1(0)	1(0)	2(1.5)**	1(1)*	2(0.5)***
4	Bile stasis	0	0(0)	0(0)	0(0.25)	0(0.25)	0(1)	0(0.25)
5	Bile duct proliferation	0	1(1.25)	3(1.5)	1(0.5)**	1(1.25)**	1(1)**	1(0.5)**
6	Kupffer cell hyperplasia	0	1(0.25)	3(1.5)*	2(0.5)	2.5(1.25)**	3(1)**	3(1.25)**†
7	Vacuolization	0	0(0.25)	1(0)	1(0.25)*	0.5(2.25)	1(2)	1(2.25)
8	Apoptosis	0	1(2)	2(1.5)**	1.5 (1.25) *	1(1.5)	1(2)	1.5(1.25) *
9	Regeneration	0	1(1.25)	1(1) $^{**\sim}$	3 (0.5) $^{**\sim}$	3.5(1) $^{**\sim}$	3(1)**†	3(1.25)$^{**\sim}$
10	Cirrhotic nodule formation	0	0(0.25)	1(0)	2(1.25)***††	2(1.5) $^{*\sim}$	1(1)$^{\#}$	1(0)
	Liver histology: Reticulin staining							
	Necrosis	0	0(1)	1(0) *	3(1.25) $^{**\sim}$	1(1) *	1(3) *	2.5(1) $^{**\sim}$

Data were presented as median (IQR) in the sham-operated and 6 experimental groups (n=7), including bile duct ligation (BDL) for 1 to 6 weeks which are abbreviated as BDL-W1, BDL-W2, BDL-W3, BDL-W4, BDL-W5, and BDL-W6. Histological changes were scored as none (0), active damage less than 25% (1), active damage less than 50% (2), active damage less than 75% (3) damage and active damage more than 75% (4)
$^{*}P<0.05$, $^{**}P<0.01$, $^{***}P<0.001$ vs Sham-Operated group, $^{\dagger}P<0.05$, $^{\dagger\dagger}P<0.01$ vs BDL-W1 group, $^{\$}P<0.05$ vs BDL-W2 group, $^{\#}P<0.05$ vs BDL-W3 group

respectively). Notably, the comparison of results among different BDL groups revealed that compared to the BDL-W2 group, the serum level of ALT was significantly increased in the BDL-W3 ($P<0.05$).

The levels of LDH were significantly increased in BDL-W1 ($P<0.01$) and BDL-W2 ($P<0.001$) compared to the sham-operated group. The most elevation in the LDH level was seen in the BDL-W2 group, so the level was significantly higher than in the first week ($P<0.05$). When compared to that of the BDL-W1, serum level of LDH was associated with a significant reduction in the BDL-W3 to W6 groups ($P<0.001$, $P<0.05$, $P<0.01$, and $P<0.01$, respectively). Additionally, the decrease in LDH levels in the BDL-W3-6 compared to the second week was significant ($P<0.001$ for all groups).

Compared to the sham-operated group, serum levels of ALP were significantly higher in all BDL groups, from the BDL-W1 to BDL-W6 ($P<0.001$, $P<0.01$, $P<0.001$, $P<0.001$, $P<0.001$, and $P<0.01$, respectively). However, comparing results among different BDL groups showed no statistically significant differences in ALP serum levels.

Histopathology

Histopathological assessment using H&E and reticulin staining is shown in Table 4 and Figures 1 and 2 (A to G).

As illustrated in Figure 1, the liver architectures were assessed for histological features using H&E staining. This evaluation encompassed the determination of vascular congestion, sinusoidal dilatation, lymphocytic infiltration, bile duct proliferation, Kupffer cell hyperplasia, vacuolization, apoptosis, regeneration, and cirrhotic nodule formation, all of which are summarized in Table 4.

Over the six-week duration, an apparent increasing pattern was observed in most parameters. However, the BDL-W2 group showed the most pronounced regeneration compared to the sham-operated ($P<0.01$) and BDL-W1 group ($P<0.05$). Furthermore, in the context of vacuolization, only the BDL-W3 group showed a statistically significant increase compared to the sham-operated group ($P<0.05$). Additionally, cirrhotic nodule formation was statistically significant in BDL-W3 and BDL-W4 in comparison with the sham-operated group ($P<0.001$ and $P<0.05$, respectively).

In the BDL-W5 and BDL-W6 groups, a notable rise in congestion was evident compared to the sham-operated group, reaching statistical significance ($P<0.01$ and $P<0.001$, respectively). Sinusoidal dilatation significantly increased in the BDL-W5 and BDL-W6 groups ($P<0.05$ and $P<0.001$, respectively). Moreover, lymphocytic cell infiltration demonstrated significant differences across BLD-W-6 compared to the sham-operated group ($P<0.01$, $P<0.05$, and $P<0.001$, respectively). There was a significant enhancement in bile duct proliferation from BDL-W3 to

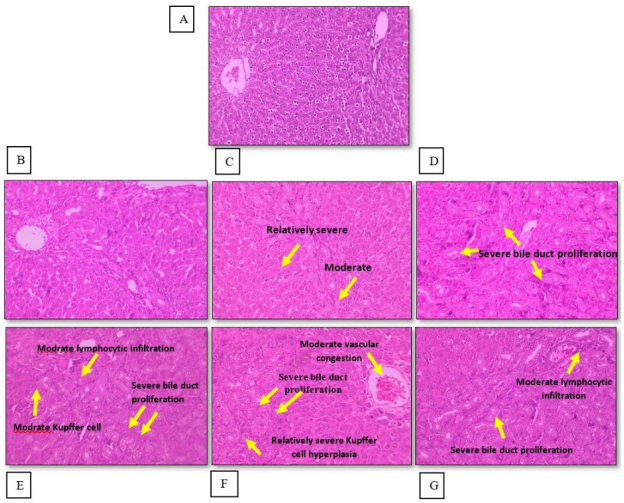

Figure 1. Light photomicrographs of histological sections of rat right liver lube (H&E staining; magnification ×400) from sham-operated group (A) and 6 experimental groups (n=7), including the bile duct ligation (BDL) for 1 to 6 weeks which are abbreviated as BDL-W1 (B), BDL-W2 (C), BDL-W3 (D), BDL-W4 (E), BDL-W5 (F), and BDL-W6 (G)

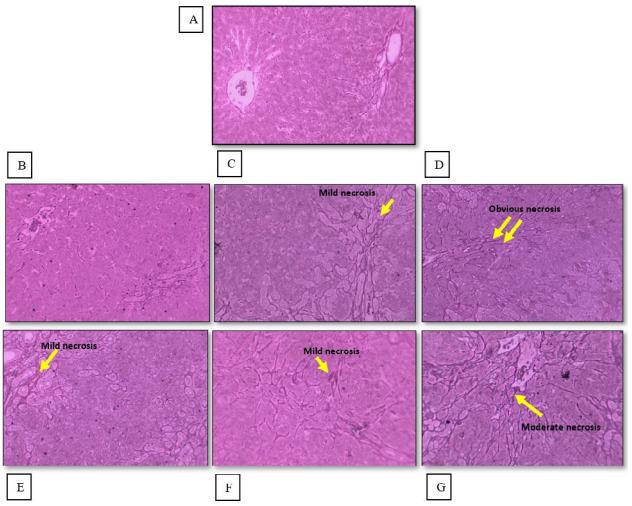

Figure 2. Light photomicrographs of histological sections of rat right liver lube (Reticulin staining; magnification ×400) from sham-operated (A) group and 6 experimental groups (n=7), including the bile duct ligation (BDL) for 1 to 6 weeks which are abbreviated as BDL-W1 (B), BDL-W2 (C), BDL-W3 (D), BDL-W4 (E), BDL-W5 (F), and BDL-W6 (G)

BDL-W6 (P<0.01) compared to the sham-operated group. Moreover, apoptosis displayed significant variations in BDL-W2 (P<0.01), BDL-W3, and BDL-W6 (P<0.05) when contrasted with the sham-operated group. Notably, there was a significant enhancement in regeneration from BDL-W2-6 (P<0.01) compared to the sham-operated group.

Molecular results

The effects of one to six weeks of bile duct ligation on hepatic gene expression are illustrated in Figures 3A-F. Compared with the sham-operated group, hepatic FXR mRNA levels were significantly down-regulated in all BDL groups, with average fold reductions of 0.258 (P<0.001), 0.674 (P=0.04), 0.538 (P=0.036), 0.572 (P=0.05), 0.376 (P<0.001), and 0.485 (P=0.05) for BDLW1 through BDLW6, respectively. The most pronounced reduction occurred at week 1. Despite the overall down-regulation of FXR, intergroup comparisons revealed significant fluctuations in expression across the six-week period; relative to BDLW1, FXR mRNA expression was significantly higher in the BDLW2, W3, and W4 groups (P<0.001, P<0.05, and P<0.05, respectively)(Figure 3A).

Measuring the mRNA expression of Nrf2 showed that compared to the sham-operated group, a significant down-regulation was observed in BDL-W2 (Figure 3B) with an average reduction fold of 0.708 (P=0.05). Moreover, between-group analysis exhibited that compared to the BDL-W1, Nrf2 mRNA expression was significantly down-regulated in BDL-W3, BDL-W4, and BDL-W5 (P<0.05 for all)(Figure 3B).

The study found that the mRNA expression of the SOD, α-GST, and GCLM genes in BDL groups was associated with some significant changes compared to the sham-operated group (Figures 3C to E). As shown in Figure 3C, in comparison with the sham-operated group, the mRNA expression of SOD in the BDL groups of W1, W3, W4, W5, and W6 (but not W2) was significantly lower, with the average reduction folds of 0.38 (P=0.006), 0.426 (P=0.008), 0.503 (P=0.04), 0.131 (P=0.04), and 0.3 (P=0.03), respectively. Notably, the expression level of BDL-W2 was significantly higher than that of BDL-W1 and BDL-W3-6 (P<0.01, P<0.01, P<0.01, P<0.05, and P<0.05, respectively). The mRNA expression of BDL-W5 was also significantly down-regulated when compared to that of BDL-W1 (P<0.05).

The mRNA expression of α-GST was significantly lower in the BDL-W1-6 groups compared to the sham-operated group, with an average reduction fold of 0.652 (P=0.003), 0.497 (P<0.001), 0.163 (P<0.001), 0.185 (P<0.001), 0.565 (P<0.001), and 0.389 (P=0.04), respectively. Notably, compared to that of BDL-W1 and W2, the mRNA expression of α-GST in BDL-W3 (P<0.001 and P<0.001) and BDL-W4 (P<0.001 and P<0.001) was significantly lower, respectively (Figure 3D).

In comparison with the sham-operated group, the GCLM mRNA in all of the BDL groups from -W1 to W6 were significantly down-regulated, with average fold reduction of 0.607 (P=0.02), 0.643 (P=0.024), 0.275 (P<0.001), 0.268 (P<0.001), 0.648 (P=0.012), and 0.31 (P=0.022), respectively (Figure 3E). Notably, the expression level in BDL-W3 was significantly lower than that of BDL-W2 (P<0.01). Moreover, the expression in the BDL-W4 was significantly lower than that of either BDL-W1 (P<0.05) or BDL-W2 (P<0.001)(Figure 3E).

Statistical analysis revealed that compared to that of the sham-operated group, the expression level of the TNF-α gene was substantially higher in all BDL groups with fold changes of 5.564 (P<0.001), 3.509 (P<0.001), 4.199 (P<0.001), 3.452 (P<0.001), 11.87 (P<0.001), and 15.87 (P<0.001) at BDL-W1 to W6, respectively (Figure 3F). Additionally, the study found that after the 4th week, the expression of the TNF-α progressively increased, so that when compared to weeks 1 to 4, the mRNA expression of TNF-α in BDL-W5 (P<0.05, P<0.001, P<0.01, and P<0.001) and BDL-W6 (P<0.05, P<0.001, P<0.01, and P<0.001) were dramatically jumped, respectively. In contrast, no considerable variations in TNF-α mRNA expression were detected between weeks 2, 3, and 4 within the BDL group.

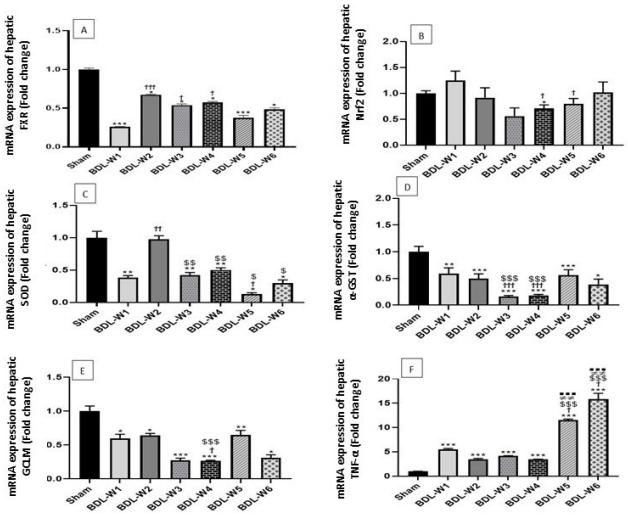

Figure 3. Effect of bile duct ligation on rat hepatic expression of FXR (A), Nrf2 (B), SOD (C), α-GST (D), GCLM (E) and TNF- α (F) in sham-operated group and 6 experimental groups (n=7), including the bile duct ligation (BDL) for 1 to 6 weeks which are abbreviated as BDL-W1, BDL-W2, BDL-W3, BDL-W4, BDL-W5 and BDL-W6

$^{*}P$<0.05, $^{**}P$<0.01, $^{***}P$<0.001 vs Sham-Operated group, $^{\dagger}P$<0.05, $^{\dagger\dagger}P$<0.01, $^{\dagger\dagger\dagger}P$<0.001 vs BDL-W1 group, $^{\$}P$<0.05, $^{\$\$}P$<0.01, $^{\$\$\$}P$<0.001 vs BDL-W2 group, $^{\#\#}P$<0.01 vs BDL-W3 group, $^{\#\#\#}P$<0.001 and vs BDL-W4 group

Discussion

In this timecourse study, we evaluated the temporal expression of key hepatic genes involved in antioxidant defense during six weeks of bile duct ligation in rats, alongside histopathological and biochemical assessments of liver injury. Our results demonstrated an overall down-regulation of FXR, SOD, αGST, and GCLM, accompanied by a transient decline in Nrf2 and a progressive up-regulation of TNF-α. FXR showed the earliest and most pronounced suppression, while αGST and GCLM were mainly reduced in the midphase of injury. In contrast, TNFα expression peaked in the later stages, consistent with the progressive inflammatory response. These findings provide a temporal overview of molecular events in BDL-induced cholestasis and highlight the potential relevance of FXR/Nrf2 modulation as a preventive or therapeutic target.

Although oxidative stress and antioxidant responses in cholestatic liver injury have been studied, most investigations have relied on single time points or isolated downstream markers. In contrast, this study was designed to map the temporal dynamics of FXR and Nrf2 signaling during the sixweek progression of BDLinduced cholestasis. By integrating molecular, biochemical, and histopathological assessments across multiple disease stages, we provide a dynamic view of how hepatic antioxidant defenses become progressively dysregulated.

FXR plays a central role in coordinating the complex processes of enterohepatic circulation and the accumulation of bile acids within liver cells (15). FXR not only suppresses the synthesis and uptake of bile acids by activating the short heterodimer partner (SHP) but also drives pathways for the detoxification of bile acids (15, 16). Notably, studies have demonstrated a significant decrease in FXR expression in individuals dealing with cholestatic conditions, encompassing progressive familial intrahepatic cholestasis 1 and 2 (PFIC1 and PFIC2), advanced stages of primary biliary cirrhosis (PBC), and biliary atresia (16-18).

Furthermore, FXR serves a metabolic function as an upstream regulator of the cellular redox state (19). This is accomplished through interactions with various downstream signaling pathways, notably the Nrf2 pathway, which plays a crucial role in the production of essential antioxidants like GSH and SOD (5, 19).

The dynamic changes observed in FXR gene expression following BDL provide intricate insights into molecular responses to cholestatic insult. The gradual decrease in Nrf2 mRNA expression, reaching a significant reduction at week 4, may reflect an extreme early cholestatic oxidative stress. The subsequent modest increase may represent a secondary phase in Nrf2 modulation involving compensatory mechanisms.

FXR exhibits a dynamic pattern, decreasing mostly in week 1, followed by fluctuating changes from week 2 to week 6. The initial decline at week 1 indicates an immediate regulatory adjustment in response to cholestasis, with subsequent dynamics suggesting a complex interplay of compensatory mechanisms. Additionally, in another previous study by Bayat *et al.*, a substantial decrease in FXR expression in the rat liver after four weeks of BDL was observed, aligning with our findings at week 4 (20). Regarding FXR expression changes in various liver diseases, multiple studies consistently demonstrate that targeting FXR has a positive influence on the better prognosis of liver injuries, encompassing conditions such as cholestasis and induced cirrhosis (6, 12, 21).

The analogous expression patterns observed for α-GST and GCLM during weeks 3 and 4 BDL indicate a coordinated response in the context of cholestatic liver injury. Both genes are integral components of the cellular antioxidant defense, with α-GST involved in detoxification processes and GCLM essential for glutathione synthesis (9). The concurrent decrease in expression for both genes during these weeks may suggest a synchronized adjustment in the cellular response to heightened oxidative stress or a shared regulatory mechanism responding to cholestasis (8). This parallel down-regulation underscores the interconnectedness of these antioxidative pathways and their joint modulation in adapting to the challenges imposed by cholestatic conditions. The coordinated changes observed in Nrf2, α-GST, and GCLM during week 4 post-BDL can be attributed to the pivotal role of the Nrf2 pathway in regulating detoxification genes. This underscores the interconnected nature of these pathways, highlighting their adaptive response to the challenges presented by cholestatic conditions (22). Moreover, the coordinated patterns of FXR and SOD expressions during BDL suggest potential correlations between metabolic and antioxidant responses. Both genes display decreases in weeks one and five, indicating synchronized regulation. The early decline in FXR and SOD at week 1 implies an immediate regulatory shift (19, 23). Changes in the serum levels of ALT and AST were slightly different throughout the experimental period. Specifically, ALT levels increased significantly in weeks 3 to 5, whereas AST levels peaked in weeks 5 and 6. Furthermore, ALP level was elevated in week 1 and remained high in weeks 3 and 4. These fluctuations in enzyme levels were paralleled by corresponding changes in the severity of histopathological changes, such as bile duct proliferation, lymphocytic infiltration, and regeneration, which were found to be associated with the down-regulation of the genes mentioned above in weeks 3 and 4.

Yang *et al.* investigated the impact of BDL on GSH synthesis and the role of specific interventions in mice. The study explores changes in the expression of GSH synthetic enzymes, specifically GCL subunits and GSH synthase, during various stages of BDL. Despite increased nuclear levels of Nrf2, a key regulator of antioxidant responses, the study observes a decline in Nrf2 nuclear binding to the antioxidant response element after 2 weeks of BDL (24).

Changes in Nrf2 expression were linked to antioxidant enzyme levels, such as GPx, SOD, and the enzyme catalase (CAT)(8, 25). These findings suggest that increased Nrf2 expression protects against oxidative stress and cell damage in the liver. Fahmy *et al.*'s study showed that antioxidant enzyme activity, including α-GST, CAT and SOD, decreased significantly after BDL surgery. They explained this by pointing to mitochondrial toxicity resulting from the accumulation of biliary acids within hepatocytes in chronic cholestasis (26).

Oxidative stress and inflammation are well-established players in developing and progressing liver fibrosis (27). The Nrf2 pathway is a critical regulator of antioxidant response element-mediated gene expression (28). It has been shown to play a crucial role in protecting hepatic cells from oxidative damage during the development of various chronic liver diseases (25). Several studies have investigated

the role of Nrf2 in liver fibrosis, with conflicting results (11, 29-31). The study found that the expression of the TNF-α gene was significantly higher in the BDL group than in the sham-operated group. The expression of this gene increased progressively over time in the BDL group, with notable differences in comparison to the sham-operated group. Specifically, the TNF-α expression level was markedly elevated in the BDL group at weeks 5 and 6.

The reduction in antioxidant enzyme gene expression suggests that BDL may lead to an imbalance between oxidants and antioxidants in the liver, which can contribute to the development of oxidative stress and tissue damage (5, 25). This is consistent with previous studies showing that BDL leads to hepatocyte injury, apoptosis, and inflammation (1, 22, 32). The increase in TNF-α gene expression suggests that BDL may activate pro-inflammatory signaling pathways, producing cytokines such as TNF-α, which regulate immune responses and tissue repair (33, 34). However, excessive or chronic production of TNF-α has been linked to various diseases, including liver cirrhosis, where it promotes fibrogenesis and hepatocellular dysfunction (35).

Conclusion

In conclusion, our study uncovered a significant alteration in the expression of FXR and its downstream Nrf2-mediated pathway in cholestatic liver injury. Notably, we observed a biphasic change in the expression of antioxidant genes, suggesting distinct phases of response to BDL. Our findings offer valuable insights into the critical periods of antioxidant gene expression, providing opportunities for targeted interventions. Strategically intervening during weeks 3 and 4 post-BDL, when the expression of these genes is most dynamic, may disrupt or modify the deleterious molecular events associated with cholestatic liver damage.

Limitations

Our results demonstrate coordinated molecular, biochemical, and histopathological changes in BDLinduced cholestasis. To further expand on these findings, future work could include proteinlevel assessments of FXR, Nrf2, and antioxidant pathways using techniques such as western blotting, immunohistochemistry, or proteomic analysis. These approaches would offer an even deeper understanding of pathway activation during BDLinduced cholestasis.

Acknowledgment

We gratefully acknowledge the laboratory technical assistance staff of the Paramedicine School of Alborz University of Medical Sciences, Iran.

Authors' Contributions

E D and EJA F contributed equally to this work. E D and EJA F designed the study; E D, EJA F, A K, and P S performed experiments and collected data; E D, EJA F, SA H, A K, and P S analyzed and interpreted results; E D and EJA F drafted the manuscript; G B and H K critically revised the manuscript and acquired funding; G B and H K supervised the project. All authors (E D, EJA F, A K, SA H, P S, G B, and H K) discussed the results, edited the manuscript, and approved the final version for publication.

Conflicts of Interest

The authors declare that they have no competing interests.

Declaration

We have not used any AI tools or technologies to prepare this manuscript.

References

1. Hirschfield GM, Heathcote EJ, Gershwin ME. Pathogenesis of cholestatic liver disease and therapeutic approaches. Gastroenterology 2010; 139: 1481-1496.
2. Cai SY, Boyer JL. The role of bile acids in cholestatic liver injury. Ann Transl Med 2021; 9: 608.
3. Li M, Cai SY, Boyer JL. Mechanisms of bile acid mediated inflammation in the liver. Mol Aspects Med 2017; 56: 45–53.
4. Schuppan D, Afdhal NH. Liver cirrhosis. Lancet 2008; 371: 838-851.
5. Petrov PD, Soluyanova P, Sánchez-Campos S, Castell JV, Jover R. Molecular mechanisms of hepatotoxic cholestasis by clavulanic acid: Role of NRF2 and FXR pathways. Food Chem Toxicol 2021; 158: 112664.
6. Petrescu AD, DeMorrow S. Farnesoid X receptor as target for therapies to treat cholestasis-induced liver injury. Cells 2021; 10: 1846.
7. Panzitt K, Zollner G, Marschall HU, Wagner M. Recent advances on FXR-targeting therapeutics. Mol Cell Endocrinol 2022; 552: 111678.
8. Yang H, Ramani K, Xia M, Ko KS, Li TW, Oh P, *et al.* Dysregulation of glutathione synthesis during cholestasis in mice: Molecular mechanisms and therapeutic implications. Hepatology 2009; 49: 1982-1991.
9. Mathan Kumar S, Dey A. Regulation of glutathione in health and disease with special emphasis on chronic alcoholism and hyperglycaemia mediated liver injury: A brief perspective. Springer Sci Rev 2014; 2: 1–13.
10. Senoner T, Schindler S, Stättner S, Öfner D, Troppmair J, Primavesi F. Associations of oxidative stress and postoperative outcome in liver surgery with an outlook to future potential therapeutic options. Oxid Med Cell Longev 2019; 2019: 3950818.
11. Galicia-Moreno M, Lucano-Landeros S, Monroy-Ramirez HC, Silva-Gomez J, Gutierrez-Cuevas J, Santos A, *et al.* Roles of Nrf2 in liver diseases: Molecular, pharmacological, and epigenetic aspects. Antioxidants 2020; 9: 980.
12. Stofan M, Guo GL. Bile acids and FXR: Novel targets for liver diseases. Front Med 2020; 7: 544.
13. Verbeke L, Mannaerts I, Schierwagen R, Govaere O, Klein S, Vander Elst I, *et al.* FXR agonist obeticholic acid reduces hepatic inflammation and fibrosis in a rat model of toxic cirrhosis. Sci Rep 2016; 6: 33453.
14. Yang Y, Chen B, Chen Y, Zu B, Yi B, Lu K. A comparison of two common bile duct ligation methods to establish hepatopulmonary syndrome animal models. Lab Anim 2015; 49: 71–79.
15. Halilbasic E, Baghdasaryan A, Trauner M. Nuclear receptors as drug targets in cholestatic liver diseases. Clin Liver Dis 2013; 17: 161-189.
16. Zollner G, Wagner M, Fickert P, Silbert D, Gumhold J, Zatloukal K, *et al.* Expression of bile acid synthesis and detoxification enzymes and the alternative bile acid efflux pump MRP4 in patients with primary biliary cirrhosis. Liver Int 2007; 27: 920–929.
17. Demeilliers C, Jacquemin E, Barbu V, Mergey M, Paye F, Fouassier L, *et al.* Altered hepatobiliary gene expressions in PFIC1: ATP8B1 gene defect is associated with CFTR downregulation. Hepatology 2006; 43: 1125–1134.
18. Alvarez L, Jara P, Sánchez-Sabate E, Hierro L, Larrauri J, Díaz MC, *et al.* Reduced hepatic expression of farnesoid X receptor in hereditary cholestasis associated to mutation in ATP8B1. Hum Mol Genet 2004; 13: 2451–2560.
19. Gai Z, Chu L, Xu Z, Song X, Sun D, Kullak-Ublick GA. Farnesoid X receptor activation protects the kidney from ischemia-reperfusion damage. Sci Rep 2017; 7: 9815.
20. Bayat G, Hashemi SA, Karim H, Fallah P, Hedayatyanfard K, Bayat M, *et al.* Biliary cirrhosis-induced cardiac abnormality in rats: Interaction between Farnesoid-X-activated receptors and the

cardiac uncoupling proteins 2 and 3. Iran J Basic Med Sci 2022; 25: 126-133.
21. Wagner M, Fickert P, Zollner G, Fuchsbichler A, Silbert D, Tsybrovskyy O, *et al*. Role of farnesoid X receptor in determining hepatic ABC transporter expression and liver injury in bile duct-ligated mice. Gastroenterology 2003; 125: 825–838.
22. Maher J, Yamamoto M. The rise of antioxidant signaling—the evolution and hormetic actions of Nrf2. Toxicol Appl Pharmacol 2010; 244: 4–15.
23. Xu Z, Tang W, Xie Q, Cao X, Zhang M, Zhang X, *et al*. Dimethyl fumarate attenuates cholestatic liver injury by activating the NRF2 and FXR pathways and suppressing NLRP3/GSDMD signaling in mice. Exp Cell Res 2023; 432: 113781.
24. Yang D, Chen X, Wang J, Lou Q, Lou Y, Li L, *et al*. Dysregulated lung commensal bacteria drive interleukin-17B production to promote pulmonary fibrosis through their outer membrane vesicles. Immunity 2019; 50: 692-706.
25. He L, Guo C, Peng C, Li Y. Advances of natural activators for Nrf2 signaling pathway on cholestatic liver injury protection: A review. Eur J Pharmacol 2021; 910: 174447.
26. Fahmy SR. Anti-fibrotic effect of Holothuria arenicola extract against bile duct ligation in rats. BMC Complement Altern Med 2015; 15: 1-12.
27. Sánchez-Valle V, C Chavez-Tapia N, Uribe M, Méndez-Sánchez N. Role of oxidative stress and molecular changes in liver fibrosis: A review. Curr Med Chem 2012; 19: 4850–4860.
28. Nguyen T, Nioi P, Pickett CB. The Nrf2-antioxidant response element signaling pathway and its activation by oxidative stress. J Biol Chem 2009; 284: 13291–13295.
29. Mohs A, Otto T, Schneider KM, Peltzer M, Boekschoten M, Holland CH, *et al*. Hepatocyte-specific NRF2 activation controls fibrogenesis and carcinogenesis in steatohepatitis. J Hepatol 2021; 74: 638–648.
30. Fuertes-Agudo M, Luque-Tévar M, Cucarella C, Martín-Sanz P, Casado M. Advances in understanding the role of NRF2 in liver pathophysiology and its relationship with hepatic-specific cyclooxygenase-2 expression. Antioxidants 2023; 12: 1491.
31. Seedorf K, Weber C, Vinson C, Berger S, Vuillard LM, Kiss A, *et al*. Selective disruption of NRF2-KEAP1 interaction leads to NASH resolution and reduction of liver fibrosis in mice. JHEP Rep 2023; 5: 100651.
32. Wen YA, Liu D, Zhou QY, Huang SF, Luo P, Xiang Y, *et al*. Biliary intervention aggravates cholestatic liver injury, and induces hepatic inflammation, proliferation and fibrogenesis in BDL mice. Exp Toxicol Pathol 2011; 63: 277–284.
33. Osawa Y, Hoshi M, Yasuda I, Saibara T, Moriwaki H, Kozawa O. Tumor necrosis factor-α promotes cholestasis-induced liver fibrosis in the mouse through tissue inhibitor of metalloproteinase-1 production in hepatic stellate cells. PloS One 2013; 8: e65251.
34. Gäbele E, Froh M, Arteel GE, Uesugi T, Hellerbrand C, Schölmerich J, *et al*. TNFα is required for cholestasis-induced liver fibrosis in the mouse. Biochem Biophys Res Commun 2009; 378: 348–353.
35. Lopetuso LR, Mocci G, Marzo M, D'Aversa F, Rapaccini GL, Guidi L, *et al*. Harmful effects and potential benefits of anti-tumor necrosis factor (TNF)-α on the liver. Int J Mol Sci 2018; 19: 2199.